Phase Boundary Calculations for Solutions of a Polydisperse Polymer

Naveen Koak and Robert A. Heidemann
Chemical and Petroleum Engineering, University of Calgary, Calgary, Alberta T2N 1N4, Canada

A technique is described for performing phase boundary calculations (cloud-point calculations) for solutions of a polydisperse polymer in a solvent component. The polymer is characterized as a potentially large number of individual components. The technique employs the Newton method for solving the nonlinear equilibrium equations. The independent variables in the equations are logarithms of the equilibrium ratios, temperature and pressure, and the mass ratio of polymer to solvent. A number of cloud-point curves were calculated using the Sanchez−Lacombe equation as the thermodynamic model. The calculations were compared with experimental data for polyethylene (M_W = 177,000 and M_N = 8,000) with n-hexane and polyethylene (M_W = 99,000 and M_N = 56,000) with ethylene. As expected, the disperse nature of the polymer significantly affected the calculated phase behavior of the polymer−solvent mixtures. Complicating features in the calculations are discussed.

Introduction

In this work we present a scheme for performing calculations for polymer/solvent systems with an equation of state when the polymer is characterized as a potentially large number of discrete pseudocomponents. The scheme uses the Newton method for solving the nonlinear equilibrium relations and is evolved from the work of Michelsen (1980) and Nghiem and Li (1984). Michelsen formulated the technique for calculation of temperature−pressure phase envelopes of multicomponent mixtures of fixed composition. Nghiem and Li extended the method to mixtures where a composition variable was significant.

The molar masses and relative amounts of the polymer pseudocomponents may be obtained from experimental molar mass distribution. However, often this information is not available, and the values of average molar masses are reported instead. In that case, the information regarding the pseudocomponents can be obtained from the experimental average molar masses, assuming an appropriate molar-mass distribution for the polymer such as the log-normal distribution proposed by Lansing and Kraemer (1935) or the Schulz distribution (Schulz, 1939). Hermitian quadrature methods can be used to define pseudocomponents from either the number-average molar mass or the mass-average molar mass, as has been discussed by Heidemann and Koak (1995).

We chose the Sanchez−Lacombe equation of state (Sanchez and Lacombe, 1976, 1978) as the thermodynamic model because of its relative computational simplicity and its ability to describe the major features of the polyethylene + *n*-hexane data of Kennis (1988), including liquid−liquid−vapor phenomena. The calculations were performed with the version of the Sanchez−Lacombe equation described by us in an earlier study (Koak and Heidemann, 1996). We presume that other equations of state (EOS) would produce behaviors similar to those shown here. The formulation of the problem is, in any case, independent of the specific EOS model.

The calculation scheme enables the rapid generation of shadow-point curves. With this procedure as a tool, it is possible to examine efficiently the effects of EOS parameters and of variations in the manner the polymer is characterized. The results presented demonstrate these effects for two significant systems involving polyethylene with ethylene and with *n*-hexane.

Two-Phase Boundary Calculations

We use z_i for the mol fraction of species i in the cloud-point phase (phase II). The composition of the incipient phase (I) (the ‘‘shadow-phase’’) is calculated from an equilibrium ratio through

$$Y_i = K_i z_i. \tag{1}$$

Correspondence concerning this article should be addressed to R. A. Heidemann.
Current address for N. Koak: Hyprotech, Ltd., Calgary, Alberta, Canada.

On convergence, the Y_i are equal to the mol fractions in the shadow phase and sum to unity; however, they are treated formally as mol numbers during the computations, and the mol fractions are found as needed through normalization.

The equilibrium requirement is

$$g_i = \left(\frac{\mu_i}{RT}\right)^{\mathrm{II}} - \left(\frac{\mu_i}{RT}\right)^{\mathrm{I}} = 0, \quad i = 1, 2, \ldots, n_c. \tag{2}$$

The Y_i should sum to unity on convergence, providing an additional equation:

$$g_{n_c+1} = \sum_{i=1}^{n_c} Y_i - 1 = \sum_{i=1}^{n_c} z_i K_i - 1 = 0. \tag{3}$$

The $n_c + 1$ functions in Eqs. 2 and 3 depend on the temperature, the pressure, and the n_c equilibrium ratios. The composition variables in the cloud-point phase, that is, the z_i, vary with the ratio of polymer to solvent.

As was proposed by Michelsen (1980), for purposes of scaling the calculations are performed using the ln K_i as the variables. We also use either $\ln T$ or $\ln P$ as a variable, depending on whether isobars or isotherms are being calculated.

Variable polymer/solvent ratio

The composition of the cloud-point phase is dealt with by introducing a variable υ, defined so that $\exp(\upsilon)$ is the mass of polymer per unit mass of solvent. This choice permits υ to range from negative infinity to positive infinity as composition varies from pure solvent to pure polymer.

For polydisperse polymers, the polymer is presumed to contain $n_c - 1$ components with individual mass fractions of m_i, $\sum_{i=2}^{n_c} m_i = 1$ and corresponding molar masses M_i, $i = 2, \ldots, n_c$; M_1 is the solvent molar mass.

On the basis of a unit mass of solvent in the cloud-point phase, the number of moles of polymer species i is

$$n_i^{II} = e^{\upsilon} \frac{m_i}{M_i}, \quad i = 2, \ldots, nc, \tag{4}$$

and therefore the polymer mol fractions in the cloud-point phase are given by

$$z_i = \frac{e^{\upsilon} m_i / M_i}{1/M_1 + \sum_{j=2}^{n_c} e^{\upsilon} m_j / M_j}. \tag{5}$$

The solvent mol fraction is

$$z_1 = \frac{m_1 / M_1}{1/M_1 + \sum_{j=2}^{n_c} e^{\upsilon} m_j / M_j}. \tag{6}$$

Newton–Raphson solution procedure

The vector of independent variables is

$$\alpha = \left(\ln K_1, \ldots, \ln K_{n_c}, \ln T \text{ or } \ln P, \upsilon\right)^T. \tag{7}$$

These $n_c + 2$ variables are available to satisfy the $n_c + 1$ conditions in Eqs. 2 and 3. Any one of the variables can be specified through an equation of the form

$$g_{n_c+2} = \alpha_s - S = 0, \tag{8}$$

where S is the specified value of the variable. At some points on a cloud-point curve, it proves to be convenient (or even essential) to be able to specify one of the K_i as being fixed.

The Newton procedure for solution is shown in vector notation by the following equations:

$$J^{(k)} \Delta \alpha^{(k)} = -g^{(k)} \tag{9}$$

$$\alpha^{(k+1)} = \alpha^{(k)} + \Delta \alpha^{(k)}, \tag{10}$$

where k is the iteration count, and J is the Jacobian matrix with elements:

$$J_{i,j} = \frac{\partial g_i}{\partial \alpha_j}. \tag{11}$$

Details of the Jacobian elements are given in the Appendix.

Initiation

Fortunately, fixing the K value of the heaviest polymer component as the specified variable α_s in Eq. 8 permits convergence of the Newton–Raphson procedure for a cloud point, even from rather poor guesses for the polymer/solvent ratio, the other K values, and the temperature or pressure. An alternative is to obtain an estimate of a cloud point through flash calculations, as described by Koak and Heidemann (1996).

Extrapolation

Once a point on the phase boundary is found, the rest of the phase boundary can be generated by taking small steps along the phase boundary. As shown by Michelsen (1980), the calculation of the phase envelope can be made more efficient and fast by fitting polynomials to a few previous points on the phase boundary to generate initial guesses for subsequent points.

At a converged point, the sensitivities of the independent variables along the cloud-point curve to a change in the one specified variable are found as the solution to:

$$J\left[\frac{\partial \alpha}{\partial S}\right]=\begin{bmatrix}0\\0\\ \vdots\\ 1\end{bmatrix}. \tag{12}$$

Linear extrapolation then takes the form;

$$\alpha_{S_2}^{(0)}=\alpha_{S_1}+\frac{\partial \alpha}{\partial S}(S_2-S_1) \tag{13}$$

for each of the independent variables. We have also experimented with fitting cubic polynomials in the specified variable to information obtained at four consecutive converged points. Michelsen (1980) points out that evaluation of the derivatives in Eq. 13 at two consecutive points is adequate to obtain a cubic extrapolation expression.

As calculations proceed, it is possible to change which of the n_c+2 variables is specified as α_s at the next point. Selecting the variable with the largest derivative $\partial\alpha/\partial S$ (in magnitude) avoids infeasible specifications that might occur at a maximum or minimum of a variable. Extrapolation with step-size control permits tracing of the whole phase boundary from an initial converged point.

Numerical difficulties

To avoid dealing with extremely low mol fractions, we remove a K value from the set of variables, unless it falls within limits such as $10^{-70}<K_j<10^{+70}$. The equilibrium condition is not satisfied for a polymer component with a K value outside the limits.

At critical points the Jacobian matrix is singular and the Newton–Raphson procedure breaks down. The success of the method in computing the whole of the cloud-point curve depends on extrapolation over critical points.

Convergence criteria

The convergence criteria used are

$$\sum_{i=1}^{n_c}[g(i)]^2\le\epsilon_g \tag{14}$$

$$\left|\sum_{i=1}^{n_c}Y_i-1\right|\le\epsilon_Y. \tag{15}$$

Quadratic convergence was observed in all cases.

Results and Discussion

Polyethylene (M_W = 99,000, M_N = 56,000) + ethylene system

Experimental data for ethylene with a number of linear polyethylenes are reported in the PhD Thesis of de Loos (1981) and in de Loos et al. (1983a). GPC data for the present polymer were converted by de Loos into a table of polymer mass amounts at 36 molar masses (de Loos, personal communication, 1998). This information is given in Table 1.

Also Figure 1 contains calculated cloud-point and shadow-phase curves using the Sanchez–Lacombe equation, in the form described by Koak and Heidemann (1996). The solid lines are the results when the de Loos 36-component characterization of the polymer is employed. In addition to the pure-component parameters, which were taken from literature sources as indicated in Table 2, there is one binary parameter available to fit data. We have used a temperature-dependent form:

$$k_{ij}=0.017378-0.00012T. \tag{16}$$

de Loos (1981) and de Loos et al. (1983b) fitted the ethylene/polyethylene data by introducing pressure dependence into the modified Flory–Huggins excess free-energy expression of Koningsveld and Kleintjens (1971). The Sanchez–Lacombe results shown in Figure 1 are comparable to those

Table 1. Characterization of Polyethylene (M_W = 99,000, M_N = 56,000)

(a) Mass Amounts and Molar Masses of 36 Polymer Components
(de Loos, personal communication)

Mass	*M*	Mass	*M*	Mass	*M*	Mass	*M*
0.08	3,300	6.33	25,900	13	86,000	6.31	198,000
0.19	4,500	7	27,900	12.8	90,000	4.01	263,000
0.32	6,000	9.13	34,200	12	109,000	3.25	3,000,000
0.8	8,200	11	42,150	11.61	110,000	2.32	350,000
1	8,800	11.84	46,000	11	118,000	1.33	470,000
1.64	10,900	13	54,000	10	132,000	0.69	625,000
2	12,300	13.54	61,000	9.5	139,000	0.3	830,000
2.56	14,400	13.82	70,000	9.03	148,000	0.15	1,500,000
4.15	19,300	13.26	82,500	8	162,000	0.1	1,700,000

(b) Mass Fractions and Molar Masses of 12 Components
(Hermitian Quadrature, Log-Normal Distribution, Match of Mn)

Mass	*M*	Mass	*M*	Mass	*M*
0.000026	2,780	0.160960	31,500	0.043903	338,300
0.000680	5,240	0.288597	56,400	0.005994	638,100
0.008148	9,650	0.286673	101,400	0.000342	1,251,000
0.049479	17,500	0.155200	183,800	0.000006	2,620,000

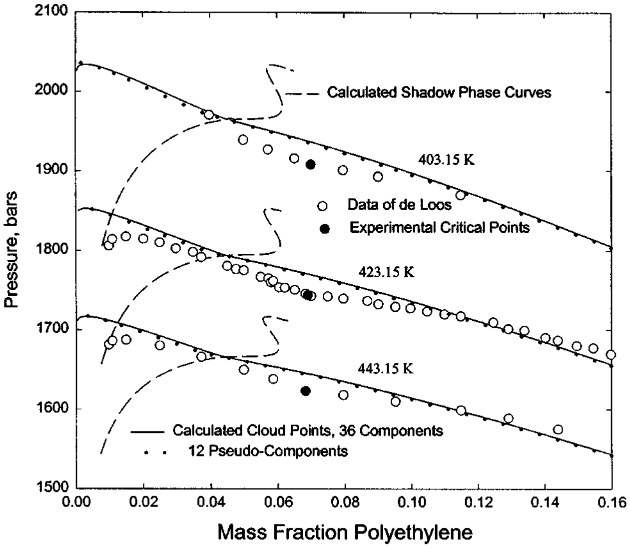

Figure 1. Experimental ethylene/polyethylene cloud-point curves (de Loos, 1981).

Calculations with a 36-component characterization and with a 12-component characterization of the polymer.

reported in the earlier work. Koak et al. (1998) have compared results using the Sanchez−Lacombe equation with computations with the SAFT equations of state.

The computational scheme makes it possible to examine variations in the way the system is modeled with relative ease. One issue of importance is whether the number of polymer components can be reduced below the 36 used by de Loos. Two approaches to reducing the number of components have been examined. In the first, the polymer has been assumed to fit the log-normal distribution and Hermitian quadrature has been used to obtain a 12-component characterization of the polymer. In this case, the number-average molar mass was the matching criterion determining quadrature points and the normalized weights were interpreted as mol fractions. The molar masses and mass fractions resulting from this process are given in Table 1b. The cloud-point curves calculated for this 12-component mixture are shown in Figure 1 as the dotted curves. These curves are virtual duplicates and lie on top of the curves calculated using the 36-component characterization of de Loos.

An alternative to quadrature as an approach to reducing the number of components is to combine them in blocks, assigning the new component the same total mass and the number average molar mass of the block. Figure 2 shows calculations for the 423.15 K isotherm. Cloud-point and shadow-phase curves are presented for characterizations with 18, 9, and 3 pseudocomponents and are compared with the original 36-component characterization. The 36-component and 18-component characterizations produce results that are very close to each other and that capture the essential nature of the experimental behavior. The 9-component and 3-component results show significant deterioration in the representation of the data. In all cases, the calculated critical point is at a lower polymer mass fraction than in the de Loos data, but this seems not to be correctable by varying the number of pseudocomponents or the interaction parameter in the Sanchez−Lacombe equation.

Table 2. Sanchez–Lacombe Equation of State Parameters

	T^* (K)	P^* (bar)	ρ^* (kg/m^3)
n-hexane**	476	2,980	775
Ethylene†	327	2,026.5	515
Polyethylene**	649	4,250	904

**Sanchez and Lacombe (1978).
†Kiszka et al. (1988).

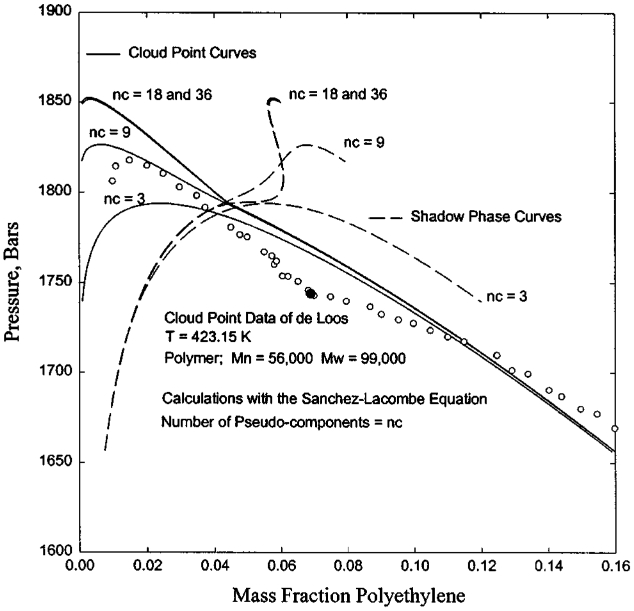

Figure 2. Effect of the number of polymer pseudocomponents on calculated cloud-point and shadow-phase curves: ethylene/polyethylene.

All the curves in Figures 1 and 2 were obtained using a cubic polynomial in the extrapolation process. Almost always, the specified variable at a point was one of the K_j equilibrium ratios. In producing these results, there was an occasional failure of the Newton−Raphson process when the critical point was approached too closely at one of the extrapolated points. However, this difficulty was removed by initiating the process with a slightly different step size.

Polyethylene (M_W = 177,000, M_N = 8,000) + n-hexane system

Kennis (1988) measured cloud-point isopleths for the preceding polyethylene in n-hexane and the data, along with a modeling effort using the Mean Field Lattice Gas equation (Kleintjens and Koningsveld, 1980), were reported by Kennis et al. (1990). We previously reported some calculations for this system (Koak and Heidemann, 1996) treating the polymer as a single component with molar mass 8,000. This polyethylene is extremely polydisperse, and a single-component characterization should not be expected to be satisfactory.

Table 3. Characterization of Polyethylene ($M_w = 177{,}000$, $M_n = 8{,}000$)

7-Component Model (Match of M_n)		3-Component Model (Match of M_w)	
Mass	M	Mass	M
0.002	128.9	0.16666667	1,699
0.0312	724.5	0.66666666	37,630
0.172	3,993	0.16666667	833,421
0.38	22,440		
0.322	134,680		
0.088	929,075		
0.005	8,800,000		

We assumed a log-normal distribution and used Hermitian quadrature to specify the molar masses and mass fractions of pseudocomponents. Heidemann and Koak (1995) describe details of the process. We have done this in two ways, the results of which are shown in Table 3. In one case, a ten-point quadrature was used in matching the number-average molar mass of 8,000. Because the polymer is extremely polydisperse, the first three pseudocomponents obtained by this method had molar masses too small to be considered as part of a polymer and were therefore discarded. The remaining mol fractions were normalized to sum to unity. The second characterization was to use only three quadrature points to match the weight-average molar mass of 177,000.

Calculations with the 3-component characterization appear in Figure 3, and the 7-component results are in Figure 4. The points shown have been reextrapolated or interpolated from the data in the Kennis (1988) thesis. In both cases, an interaction parameter of $k_{ij} = -0.10$ was found to provide a rough match of the data. It appears that no single interaction parameter with this model could provide a quantitative fit of these data. However, the 6-bar vapor cloud point is matched, and each of the isotherms cuts across the experimental data. Also, the general shape of the calculated shadow-phase curves is correct.

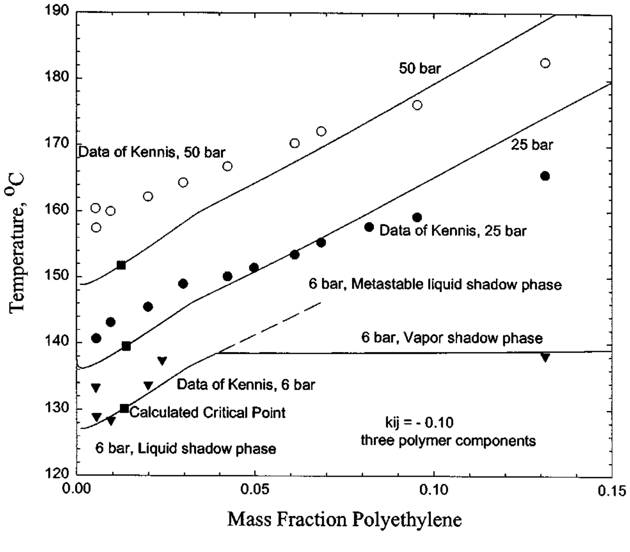

Figure 3. Cloud-point isobars for *n*-hexane/polyethylene using 3 polymer pseudocomponents: Hermitian quadrature to match M_w.

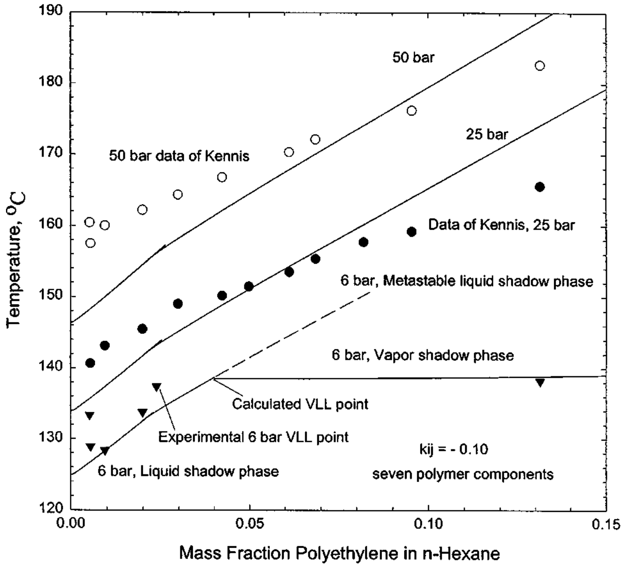

Figure 4. Cloud-point isobars for *n*-hexane/polyethylene using 7 polymer pseudocomponents: ten-point Hermitian quadrature to match M_n.

The system shows three-phase VLLE behavior at the lowest pressure. Some of the Kennis data, as noted, are for cloud points with a hexane-rich vapor as the shadow phase. The technique for finding the liquid–liquid and vapor–liquid 6-bar lines separately requires only the specification of which volume root to choose from the equation of state when three were found.

A close examination of each isotherm in Figure 4 reveals a self-crossing at a low polymer mass fraction. The details of the 50-bar line are shown in Figure 5. Along the cloud-point line (and the corresponding shadow-phase line), the parameter that is varying continuously is the K equilibrium ratio for the heaviest component, with a molar mass of 8.8×10^6. Its K value decreases from 9.0 to 5×10^{-56} in the composition range shown in Figure 5. Cusps occur in the cloud-point curve where the polymer mass fraction and the temperature simultaneously pass through a maximum or a minimum. The curve for the shadow phase passes a minimum and a maximum at the two points.

The cloud-point line can be seen to cross itself. At this intersection, there are two different shadow phases in equilibrium with a polymer/solvent mixture of a fixed composition. For this reason, the point is labeled on the figure as a three-phase point, where all three phases are liquids. The apparent critical point for this isobar, that is, the point where all the K values are unity, occurs inside the two-phase region at a point where the polymer-hexane solution is locally unstable. Šolc (1970) described similar behavior in calculated cloud points. His analysis concludes that all the features observable in Figure 5 result when the polymer is highly polydisperse.

Most of the calculations summarized in Figures 3–5 were performed using linear extrapolation (Eqs. 12 and 13) to initiate the next point from a converged calculation. In most cases, the specified variable was one of the equilibrium ratios. The

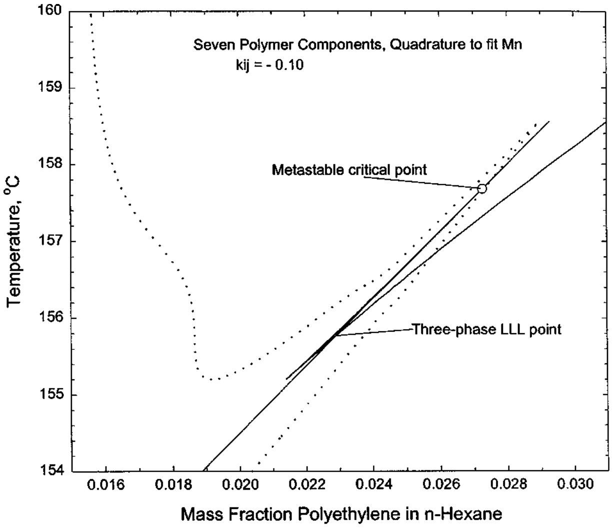

Figure 5. Detail of the 50-bar isobar in Figure 4.

It shows a self-crossing, a three-phase liquid–liquid–liquid equilibrium point, and an unstable critical point.

folded cloud-point curve in Figure 5 could not easily have been found by specifying the polymer mass fraction, since the equations clearly have three different solutions in the region of interest.

Summary

The approach described in this article for cloud-point calculations requires a Newton–Raphson solution of a set of nonlinear equations. It enables rapid calculation of phase boundaries of highly nonideal polymer–solvent systems, even when there are many polymer components. The ethylene/polyethylene example involves 36 polymer pseudocomponents.

Our results show that the polydispersity of the polymer is an important issue. The computational procedure enables an examination of alternative ways to characterize a polydisperse polymer. The *n*-hexane/polyethylene example exposes the possibility of 3-phase liquid–liquid–liquid equilibria resulting from polydispersity. Such complications are handled as a matter of course in the computational process.

Acknowledgment

This research was supported by a grant from the Natural Sciences and Engineering Research Council of Canada.

Notation

J = Jacobian matrix
g_i = function to be zero at a cloud point
K_i = distribution coefficient of component i
k_{ij} = binary interaction parameter for the i, j pair
m_i = mass fraction of a component in the polymer, $i = 2, \ldots, n_c$
M_i = molar mass of component i; the solvent is component 1
M_n = number-average molar mass
M_w = weight-average molar mass
n_c = number of components, solvent plus polymer species
n_j = number of moles of component j
n_T = total number of moles in a phase
P = pressure
P^* = Sanchez-Lacombe parameter
R = gas constant
S = specified value
T = temperature
T^* = Sanchez-Lacombe parameter
v = polymer mass variable
w_1 = mass fraction of solvent in the cloud-point phase, II
y_i = mol fraction of component i in the shadow phase, I
Y_i = mol number of component i in the shadow phase, I
z_i = mol fraction of component i in the cloud-point phase, II

Greek letters

α_i = component of the variable vector
α = variable vector
$\Delta\alpha$ = correction vector
μ_i = chemical potential of component i
ρ = Sanchez-Lacombe parameter

Subscripts and superscripts

I, II = phase indices
i, j, k = component indices
(k) = iteration count
s = specified variable

Literature Cited

De Loos, Th. W., “Fluid Phase Equilibrium in Systems of Linear Polyethylene and Ethylene,” PhD Thesis, Technical Univ. of Delft, Delft, The Netherlands (1981).

De Loos, Th. W., W. Poot, and G. A. M. Diepen, “Fluid Phase Equilibria in the System Polyethylene + Ethylene. 1. Systems of Linear Polyethylene + Ethylene at High Pressure,” *Macromolecules*, **16**, 111 (1983a).

De Loos, Th. W., R. N. Lichtenthaler, and G. A. M. Diepen, “Fluid Phase Equilibria in the System Polyethylene + Ethylene. 2. Calculation of Cloud Point Curves for Systems of Linear Polyethylene + Ethylene,” *Macromol.*, **16**, 117 (1983b).

Heidemann, R. A., and N. Koak, Letter to the Editor, *AIChE J.*, **41**, 737 (1995).

Kennis, H. A. J., “The Influence of Nitrogen on the Phase Behavior of the System *n*-Hexane/Linear High Density Polyethylene,” PhD Thesis, Technical Univ. of Delft, The Netherlands (1988).

Kennis, H. A. J., Th. W. de Loos, J. de Swaan Arons, R. Van Der Haegen, and L. A. Kleintjens, “The Influence of Nitrogen on the Liquid-Liquid Phase Behavior of the System *n*-Hexane-Polyethylene: Experimental Results and Predictions with the Mean-Field Lattice-Gas Model,” *Chem. Eng. Sci.*, **45**, 1875 (1990).

Kiszka, M. B., M. A. Meilchen, and M. A. McHugh, “Modeling High-Pressure Gas-Polymer Mixtures Using the Sanchez–Lacombe Equation of State,” *J. Appl. Poly. Sci.*, **36**, 583 (1988).

Kleintjens, L. A., “The Influence of Nitrogen on the Liquid-Liquid Phase Behavior of the System n-Hexane-Polyethylene: Experimental Results and Predictions with the Mean-Field Lattice-Gas Model,” *Chem Eng. Sci.*, **45**, 1875 (1990).

Kleintjens, L. A., and R. Koningsveld, “Liquid-Liquid Phase Separation in Multicomponent Polymer Systems. XIX. Mean Field Lattice-Gas Treatment of the System *n*-Alkane/Linear-Polyethylene,” *Colloid Poly. Sci.*, **258**, 711 (1980).

Koak, N., and R. A. Heidemann, “Polymer-Solvent Phase Behavior Near the Solvent Vapor Pressure,” *Ind. Eng. Chem. Res.*, **35**, 4301 (1996).

Koak, N., R. M. Visser, and Th. W. de Loos, “High-Pressure Phase Behavior of Some Polymer-Solvent Systems,” Int. Conf. on Fluid Properties and Phase Equilibria for Chemical Process Design, The Netherlands (1998).

Koningsveld, R., and L. A. Kleintjens, “Liquid-Liquid Phase Separation in Multicomponent Polymer Systems: X. Concentration Dependence of the Pair Interaction Parameter in the System Cyclohexane-Polystyrene," *Macromolecules*, **4**, 637 (1971).

Lansing, W. D., and E. O. Kraemer, "Molecular Weight Analysis of Mixtures by Sedimentation Equilibrium in the Svedberg Ultracentrifuge," *J. Amer. Chem. Soc.*, **57**, 1369 (1935).

Michelsen, M. L., "Calculation of Phase Envelopes and Critical Points for Multicomponent Mixtures," *Fluid Phase Equilib.*, **4**, 1 (1980).

Nghiem, L. X., and Y.-K. Li, "Computation of Multiphase Equilibrium Phenomena with an Equation of State," *Fluid Phase Equilib.*, **17**, 77 (1984).

Sanchez, I. C., and R. H. Lacombe, "An Elementary Molecular Theory of Classical Fluids. Pure Fluids," *J. Phys. Chem.*, **80**, 2352 (1976).

Sanchez, I. C., and R. H. Lacombe, "Statistical Thermodynamics of Polymer Solutions," *Macromolecules*, **11**, 1145 (1978).

Schulz, G. V., "Uber die Kinetik der Kettenpolymerisation," *Z. Phys. Chem., B*, **43**, 25 (1939).

Šolc, K., "Cloud Point Curves of Polymer Solutions," *Macromolecules*, **3**, 665 (1970).

Appendix

The derivatives of the equilibrium function with respect to the $\ln K$ variables are

$$\left(\frac{\partial g_i}{\partial \ln K_j}\right)_{T,P} = -\,y_j\left[n_T\frac{\partial \mu_i/RT}{\partial n_j}\right]^{\mathrm{I}}_{T,P}, \qquad i=1,\ldots,n_c, \quad j=1,\ldots,n_c. \quad \text{(A1)}$$

Similarly, standard identities lead to

$$\frac{\partial g_i}{\partial v} = -\,z_1\left[n_T\frac{\partial \mu_i/RT}{\partial n_1}\right]^{\mathrm{II}}_{T,P} + y_1\left[n_T\frac{\partial \mu_i/RT}{\partial n_1}\right]^{\mathrm{I}}_{T,P}, \qquad i=1,\ldots,n_c. \quad \text{(A2)}$$

The derivatives at constant temperature and pressure must be found from the chain rule:

$$n_T\left[\frac{\partial \mu_i/RT}{\partial n_j}\right]_{T,P} = \frac{n_T}{RT}\,\frac{\left(\frac{\partial P}{\partial n_i}\right)_{T,V}\left(\frac{\partial P}{\partial n_j}\right)_{T,V}}{\left(\frac{\partial P}{\partial V}\right)_T} + n_T\left(\frac{\partial \mu_i/RT}{\partial n_j}\right)_{T,V}. \quad \text{(A3)}$$

These derivatives are written in terms of the total volume and the numbers of moles (that is, the convenient variables for mechanical differentiation), but the results can be expressed in terms of the molar volume and the mol fractions.

The other derivatives involved in the computation are

$$\left(\frac{\partial g_i}{\partial \ln T}\right)_{K,P} = T\left[\left(\frac{\partial \mu_i/RT}{\partial T}\right)^{\mathrm{II}}_{z,P} - \left(\frac{\partial \mu_i/RT}{\partial T}\right)^{\mathrm{I}}_{Y,P}\right], \qquad i=1,\ldots,n_c \quad \text{(A4)}$$

$$\left(\frac{\partial g_i}{\partial \ln P}\right)_{K,T} = \frac{P}{RT}\left[\left(\frac{\partial V}{\partial n_i}\right)^{\mathrm{II}}_{T,P} - \left(\frac{\partial V}{\partial n_i}\right)^{\mathrm{I}}_{T,P}\right], \qquad i=1,\ldots,n_c, \quad \text{(A5)}$$

where

$$\left(\frac{\partial V}{\partial n_i}\right)_{T,P} = -\,\frac{(\partial P/\partial n_i)_{T,V}}{(\partial P/\partial V)_T} \quad \text{(A6a)}$$

$$\left(\frac{\partial g_{n_c+1}}{\partial \ln K_j}\right)_{T,P} = Y_j, \qquad j=1,\ldots,n_c \quad \text{(A6b)}$$

$$\left(\frac{\partial g_{n_c+1}}{\partial \ln T}\right)_{K,P} = 0 \quad \text{(A7)}$$

$$\left(\frac{\partial g_{n_c+1}}{\partial \ln P}\right)_{K,T} = 0 \quad \text{(A8)}$$

$$\frac{\partial g_{n_c+1}}{\partial v} = z_1\left(\sum_{i=1}^{nc} Y_i - K_1\right). \quad \text{(A9)}$$

Manuscript received Oct. 6, 1999, and revision received Sept. 28, 2000.